STEMedicine

RESEARCH ARTICLE

Anethole attenuates lung cancer progression by regulating the proliferation and apoptosis through AKT and STAT3 signaling

Venkata Kumar and Maddula Venkateswarulu*

Maharishi Markandeshwar Institute of Medical Science and Research, Mullana, Haryana, India

Abstract

***Background*:** The main constituent of fennel, anethole, exerts beneficial effects in many diseases, including antiproliferative and tumoricidal capacities. This study aimed to investigate the effect of anethole on the human non-small cell lung cancer (NSCLC) cell line, A549, and the related molecular mechanisms.
***Methods*:** The proliferation was assessed by 3-(4,5-Dimethylthiazol-2-yl)-2,5-diphenyltetrazolium bromide and colony formation assays. Apoptosis situation was determined using fluorescence-activated cell sorting and DNA fragmentation assay combined with immunoblotting assay probing-related protein expression. Phosphoinositide 3-kinases-protein kinase B (PI3K-AKT) and signal transducer and activator of transcription 3 (STAT3) signaling proteins were evaluated using immunoblotting. Xenograft model was constructed to determine the tumor volume and weight and to evaluate the expression of Ki67 via immunohistochemistry and cleaved caspase 3 via immunoblotting.
***Results*:** Anethole inhibited proliferation and clonal growth of A549 cells. The promotion of A549 cell apoptosis by anethole was evidenced by increased apoptotic ratio, abundant DNA fragments, and caspase-3 activation. Key proteins in PI3K-AKT and STAT3 signaling pathways were decreased in anethole group. Additionally, xenografted tumors in anethole group retarded with decreased Ki67 and increased cleaved caspase 3 expression.
***Conclusions*:** Anethole induced tumor cell apoptosis and retarded cell proliferation. AKT and STAT3 signaling pathways might be involved in the effects of anethole. Our findings highlight the feasibility of anethole in the treatment of lung cancer.

Keywords: *anethole*; *lung cancer*; *apoptosis*; *STAT3*

Received: 16 November 2022; Revised: 24 November 2022; Accepted: 25 November 2022; Published: 11 January 2023

Etiological studies of lung cancer have been focused on smoking and environmental pollution along with genetic factors (1, 2). Histologically, lung cancer is composed of two subtypes: non-small lung cancer (NSCLC) and small cell lung cancer (SCLC) (3). The majority of NSCLC cases is diagnosed at advanced stages of cancer, which is insensitive to most antitumor therapies and contributes to the high morbidity of lung cancer in many countries, especially the developing ones (3).

Conventional treatments for lung cancer include radiotherapy, chemotherapy, surgery as well as immunotherapy, among which chemotherapy is of the predominant importance (4, 5), while the severe side effects correlated with chemotherapeutic choices could not be ignored, such as fatigue, bleeding, gastrointestinal reactions, kidney and liver dysfunction, bone marrow suppression, and so on (6–8). Hence, finding more safe and effective chemotherapeutic agents is extraordinarily urgent now.

Anethole is the main flavoring component of essential oils usually extracted from anise, star anise, and sweet fennel (9). Previous studies indicated that anethole possesses extensive pharmacological effects in disease therapy, such as anti-inflammatory, neuroprotective, antidiabetic, immunomodulatory as well as antithrombotic effects (9). Anethole suppresses the migration and proliferation of prostate cancer cells and breast cancer cells while accelerates cell apoptosis (10, 11). Anethole suppresses NF-κB activation to block tumor necrosis factor transduced cellular responses (12). PI3K/AKT and signal transducer

†These authors are equal contribution to this work

Citation: STEMedicine 2023, 4(1): e153 - http://dx.doi.org/10.37175/stemedicine.v4i1.153

and activator of transcription 3 (STAT3) signaling pathways have been reported to be involved in the antitumor process of anethole (13). The role of anethole on lung cancer has not been illustrated yet.

Since anethole has exhibited inhibitory effects on various types of cancers, we hypothesized that it might exert antitumor effects on lung cancer.

Methods and materials

Cell culture

NSCLC cell line A549 cells were obtained from the ATCC (Manassas, VA). A549 cells were cultured in Roswell Park Memorial Institute-1640 medium (Hyclone, Logan, UT) supplemented with 10% fetal bovine serum (FBS, Hyclone) and 1% penicillin/streptomycin solution (Sigma Aldrich, St. Louis, MO) at 37°C, 5% CO_2.

Drug preparation

For in vitro assays, anethole power (anethole, MedChemExpress, Monmouth Junction, NJ) was dissolved in dimethyl sulfoxide (DMSO). For in vivo assays, anethole power was dissolved to make a stock solution of 6.25 mg/ml by sequentially adding DMSO (10% in the final solution) and corn oil (90% in the final solution). All the stock solutions were placed at −80°C for long-term storage.

Cell proliferation assessment

3-(4,5-Dimethylthiazol-2-yl)-2,5-diphenyltetrazolium bromide (MTT) as well as colony formation assays was employed to evaluate cell proliferation.

For MTT assay, A549 cells were plated into the culture plates at the density of 3,500 cells per well for 24 h before treatment with anethole of indicated concentrations (0, 25, and 50 μM). After incubating for 24, 48, or 72 h, MTT solution (10 μL, 5 mg/mL in phosphate-buffered saline (PBS), Sigma Aldrich) was added and incubated the cells at 37°C for 4–5 h. The absorbance at 570 nm was measured using a microplate reader.

Colony formation assay was conducted using Giemsa staining. Cells were seeded into 6-well plates at the concentration of 500 cells per well for 24 h before treatment with 50 μM anethole. Then, the cells were washed with sterile PBS once and stained with Giemsa solution. The number of colonies were counted.

Cell apoptosis detected by flow cytometry

After the cells were treated with indicated concentrations of anethole for 48 h, they were collected after trypsin digestion. Then, cells were resuspended in PBS with 2% FBS on ice, followed by the addition of Annexin V-fluorescein isothiocyanate and propidium iodide (PI). Cell apoptosis was detected using a flow cytometer (Beckman Coulter, Brea, CA).

Western blot

Cells were lysed using radioimmunoprecipitation lysis buffer with protease inhibitor (Thermo Waltham, MA). Equal amount (20 μg) of protein in each group was loaded and separated using sodium dodecyl sulfate–polyacrylamide gel electrophoresis and then transferred onto a polyvinylidene fluoride membrane. They were further incubated with primary antibodies at 4°C overnight. The primary antibodies include anti-glyceraldehyde-3-phosphate dehydrogenase (GAPDH) antibody (MA#2118; CST, San Diego, CA; 1:5000), anti-Cleaved Caspase 3 antibody (#9661; CST; 1:1000), anti-BCL2 Antagonist/Killer (BAK) antibody (#3814; CST; 1:2000), anti-bcl-2-like protein (BAX) antibody (#2772; CST; 1:2000), anti-B-cell lymphoma 2 (BCL-2) antibody (12789-1-AP; Proteintech, Chicago, IL, USA; 1:1000), anti-myeloid cell leukemia-1 (MCL-1) antibody (#5453; CST; 1:1000), anti-p-AKT antibody (#9271; CST; 1:1000), anti-AKT antibody (#9272; CST; 1:2000), anti-Stat3 antibody (#9139; CST; 1:3000), anti-p-Stat3 antibody (#9145; CST; 1:1000), anti-PI3K antibody (#4228; CST; 1:2000), and anti-p-PI3K antibody (#4257; CST; 1:1000). GAPDH served as inner control.

DNA fragmentation electrophoresis

After treatments by different concentrations of anethole for 48 h, cells were collected using trypsin digestion. Equal numbers of cells (about 5×10^6 cells) for each group was suspended in 500 μL Tris–ethylenediaminetetraacetic acid (EDTA) with 0.2% Triton X-100 for 30-min dissociation. Then, cell lysates were precipitated in ethanol with 0.5 M NaCl for 6 h and extracted using phenol-chloroform. Next, isopropanol was added into the mixture before placing at −20°C for 2 h. Afterward, the pellet collected was re-suspended in Tris-EDTA solution and digested in Rnase A at 37°C for 35 min. Finally, the DNA fragments were separated by 1% agarose gel.

Tumor xenograft

BALB/c nude mice (18–22 g) were fed *ad libitum*. All animals involved in experiments in this study were performed under the approval of Maharishi Markandeshwar Institute of Medical Science and Research. A549 cells were inoculated subcutaneously in the dorsal flanks of mice at the volume of 3×10^6/site. Two weeks later, those with tumor volume of 100 mm^3 were selected for further drug treatment. Then, mice were treated by vehicle, 25 or 50 mg/kg anethole via oral gavage daily for 25 consecutive days. On day 25, animals were sacrificed, and xenografted tumors were collected, weighed, and subjected to immunohistochemistry.

Immunohistochemistry

After fixation in 10% neutral formalin at 4°C for 24 h followed by dehydration in gradient concentrations of alcohol, samples were cut into 4-μm sections. Then, 0.3% hydrogen

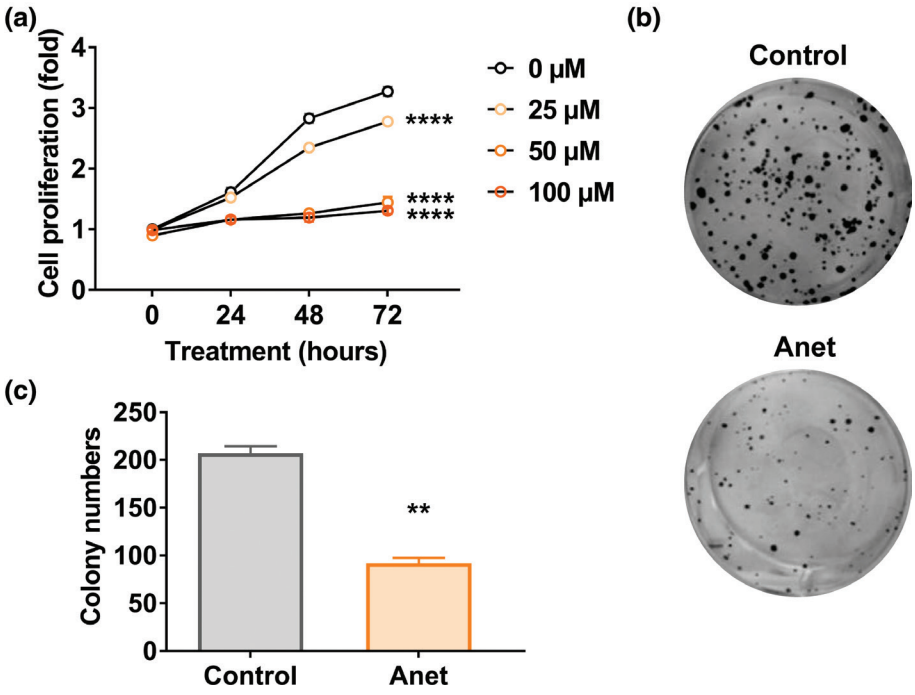

Fig. 1. Anethole inhibited the proliferation of A549 cells. (a) A549 cells were treated with anethole at the indicated concentrations for the indicated times, and cell proliferation was determined by MTT assay. (b and c) Colony formation assay of A549 cells under the treatment of vehicle or 50 μM anethole was conducted to examine the effect of anethole on the proliferation of A549 cells. Four replicated wells for each condition. Error bar represents SEM. $^{**}P < 0.01$ and $^{****}P < 0.0001$.

peroxide was applied to block endogenous peroxidase activity. The sections were blocked by 5% normal goat serum at room temperature for 30 min and probed with anti-Ki67 antibody (1:500; ab21700; Abcam, Cambridge, MA, USA) at 4°C overnight. Elivision super HRP (Mouse/Rabbit) IHC Kit (Maixin-Bio, Shenzhen, China) as well as 3, 3'-diaminobenzidine was utilized to visualize the reaction; meanwhile, hematoxylin was administered to visualize nuclei. Ethanol was used for the dehydration of the final sections before mounting with neutral resins (Solarbio).

Statistics

Data were analyzed using two-tailed *t*-test, two-way analysis of variance (ANOVA) test, or one-way ANOVA with Tukey's multiple-comparisons test. Error bar represents standard error of mean (SEM).

Results

Anethole inhibited the proliferation of A549 cells

As shown in Fig. 1a, A549 cell proliferation was inhibited by low dose of anethole (25 μM) at the 48-h and 72-h time point. Noteworthy, moderate and high doses of anethole (50 and 100 μM) sharply inhibited A549 cell proliferation at all time points. Furthermore, moderate to high concentrations of anethole exerted similar inhibitory effects on A549 cells, which was further confirmed using colony formation assay. It was demonstrated that the colonies formed in 50-μM group were significantly less than those in the control group (Fig. 1b, c). These two experiments co-suggest that anethole exerts inhibitory effects on A549 cells, which provide a solid base for the following study.

Anethole promoted the apoptosis of A549 cells

Fluorescence-activated cell sorting (FACS) and DNA fragmentation combined with immunoblotting assays were used to evaluate the effects of anethole on apoptosis of A549 cells. FACS assay revealed that the ratio of apoptotic cells was significantly increased by anethole dose-dependently (Fig. 2a, b). As shown in Fig. 2c and d, DNA fragments were obviously abundant in A549 cells after anethole treatment in a dose-dependent manner, indicating anethole promote apoptosis of A549 cells. In Fig. 2e and f, the detection of apoptotic effector protein, cleaved caspase 3, showed an obvious increased expression of cleaved caspase 3 in anethole-treated A549 cells dose-dependently, further confirming the promotion of anethole on the apoptosis of A549 cells.

Anethole regulated the expression of apoptosis-related proteins in A549 cells

To further explore the apoptosis-related response of A549 cells after anethole treatment, the apoptosis-related proteins of cells treated by anethole for indicated times (0, 12, and

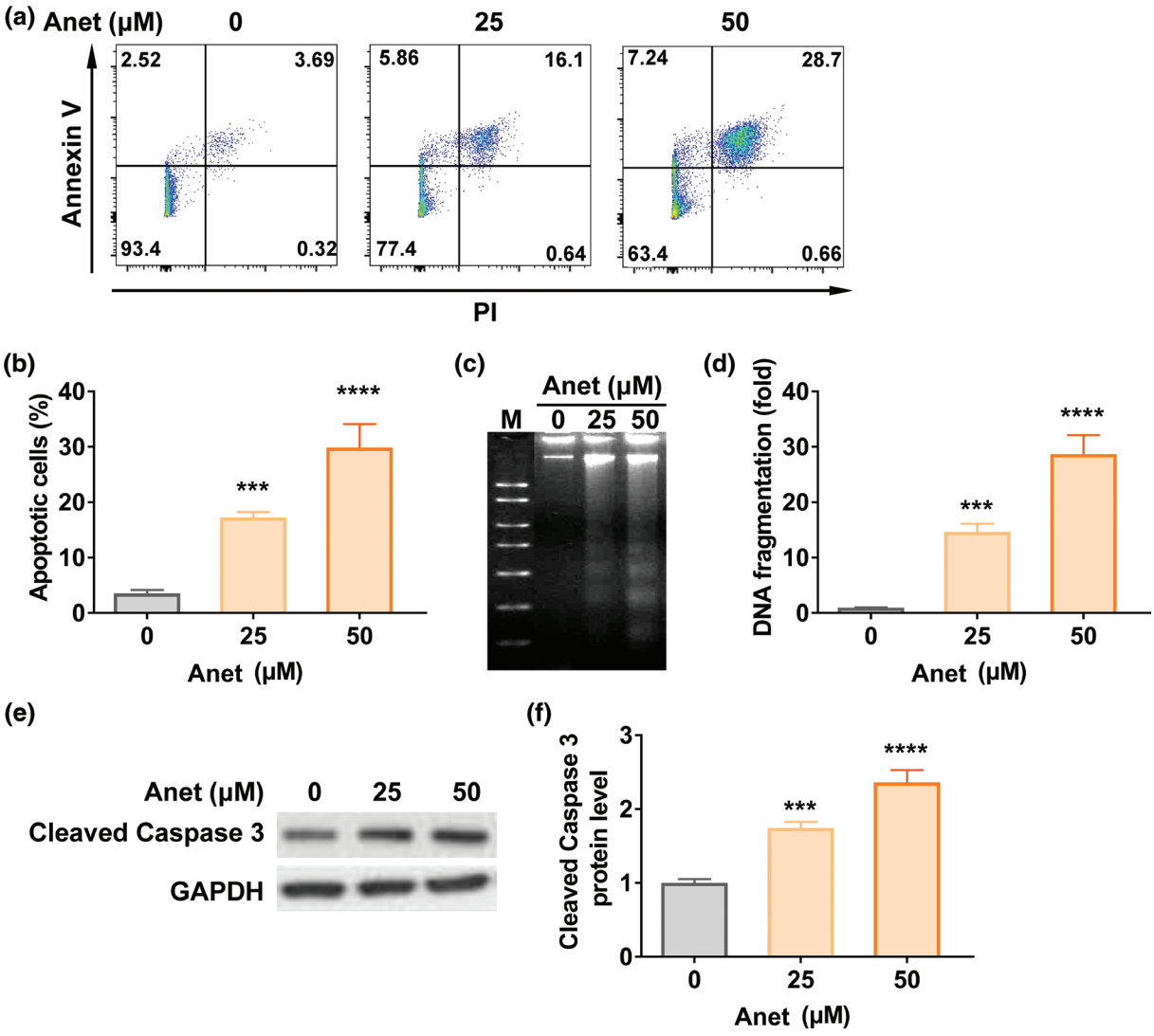

Fig. 2. Anethole promoted the apoptosis of A549 cells. A549 cells were treated with anethole at the indicated concentrations for 48 h, and cell apoptosis was determined by FACS (a and b), DNA fragmentation (c and d), and the immunoblotting assays (e and f). Four replicated wells were designed for each condition. Error bar represents SEM. $^{***}P < 0.001$ and $^{****}P < 0.0001$.

24 h) were detected. Here, the dose of 50 μM was adopted for its highest antitumor effect on A549 cells. Western blot assay showed that, compared with the control group, medium dosage of anethole markedly enhanced the expression of proapoptotic BAK (Fig. 3a, b) and BAX (Fig. 3a, c), whereas it reduced antiapoptotic BCL2 (Fig. 3a, d) and MCL1 (Fig. 3a, e) in A549 cells in a time-dependent manner.

Anethole regulated AKT and STAT3 signaling in A549 cells

To explore the possible molecular mechanisms underlying the antitumor effects of anethole in A549 cells, the expression of the two pathway-related proteins was analyzed 6 h after anethole treatment (0, 25, and 50 μM). As shown in immunoblotting assay, the protein levels of p-PI3K (Fig. 4a, b), p-AKT (Fig. 4a, c), and p-STAT3 (Fig. 4a, d) were all significantly decreased compared with those in the vehicle control group, indicating that the observed effects may be via downregulating Phosphoinositide 3-kinases-protein kinase B (PI3K-AKT) and STAT3 pathway effectors.

Anethole inhibited tumor progression

Furthermore, we verified whether anethole exerted inhibitory effects on A549 cells in vivo in order to echo the above *in vitro* findings. Mice with xenografted tumor were treated by indicated doses of anethole for 25 days. As shown in Fig. 5a, curves of tumor volume rose over time in three groups, and anethole obviously decreased the tumor volume dose-dependently. Compared with the vehicle control group, anethole also significantly decreased the tumor weight in a dose-dependent manner (Fig. 5b).

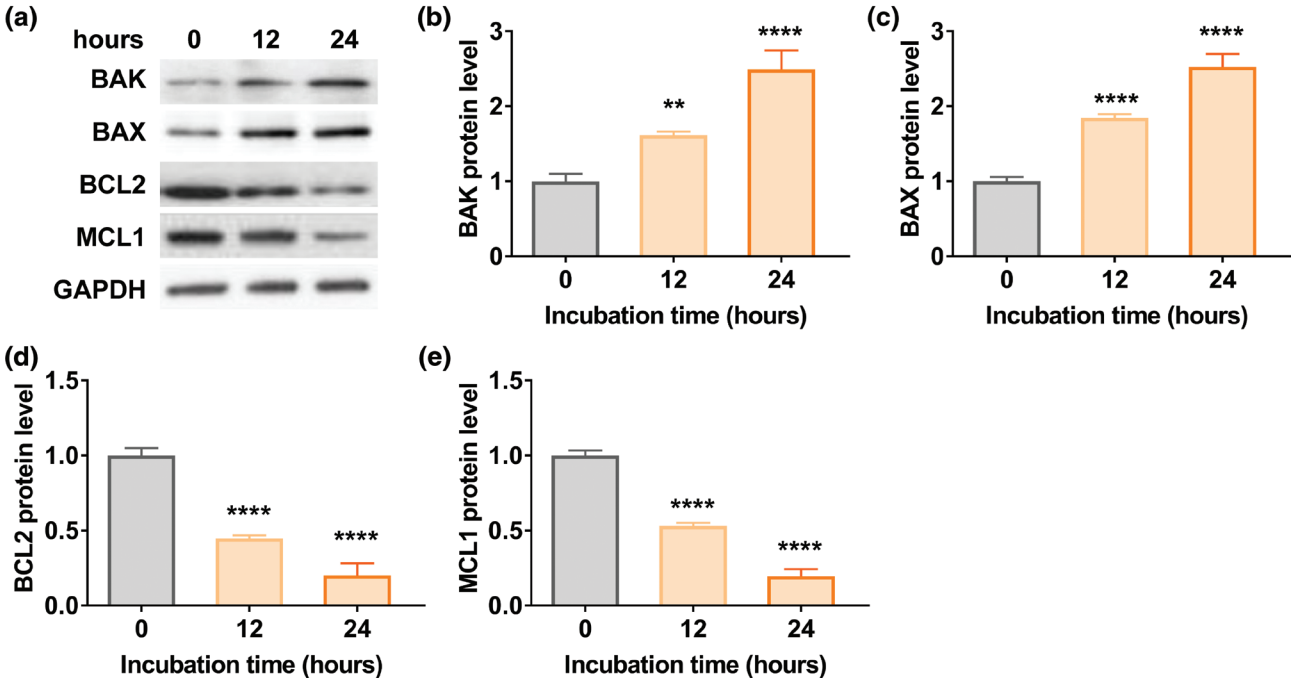

Fig. 3. Anethole regulated the expression of apoptosis-related proteins in A549 cells. A549 cells were treated with 50 μM anethole for indicated times, and then cells were harvested to determine the protein levels of BAK (a and b), BAX (a and c), BCL2 (a and d), and MCL1 (a and e) by Western blot. Four replicated wells for each condition were performed. Error bar represents SEM. $^{**}P < 0.01$ and $^{****}P < 0.0001$.

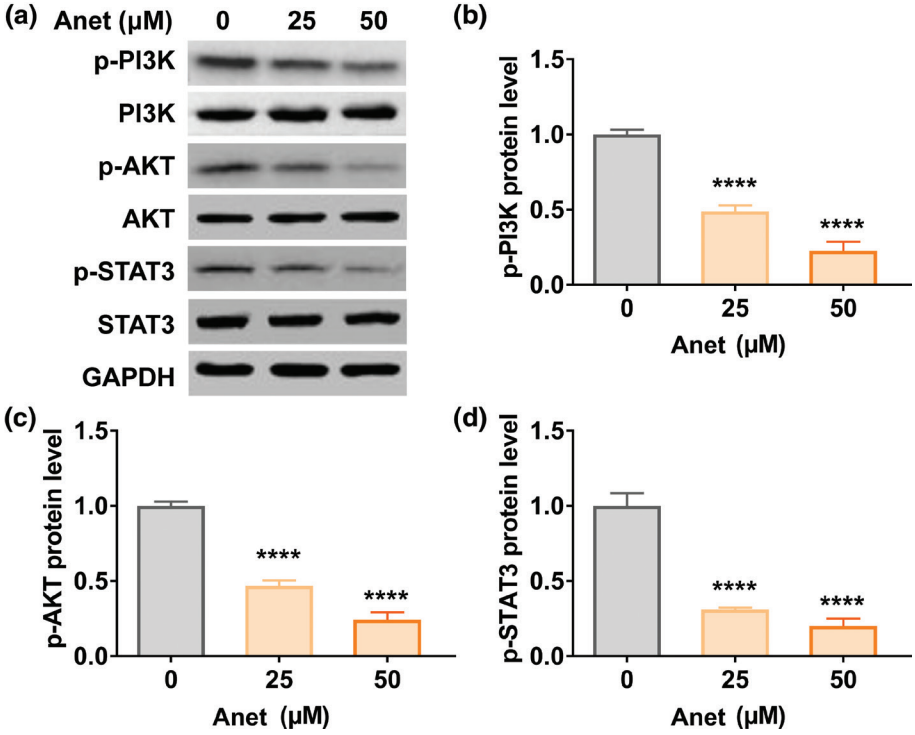

Fig. 4. Anethole regulated AKT and STAT3 signaling in A549 cells. A549 cells were treated with vehicle, 25, or 50 μM anethole for 6 h and then harvested to analyze the protein level of p-PI3Kp85α (a and b), p-AKT (a and c), and p-STAT3 (a and d) by Western blot. Four replicated wells for each condition. Error bar represents SEM. $^{****}P < 0.0001$.

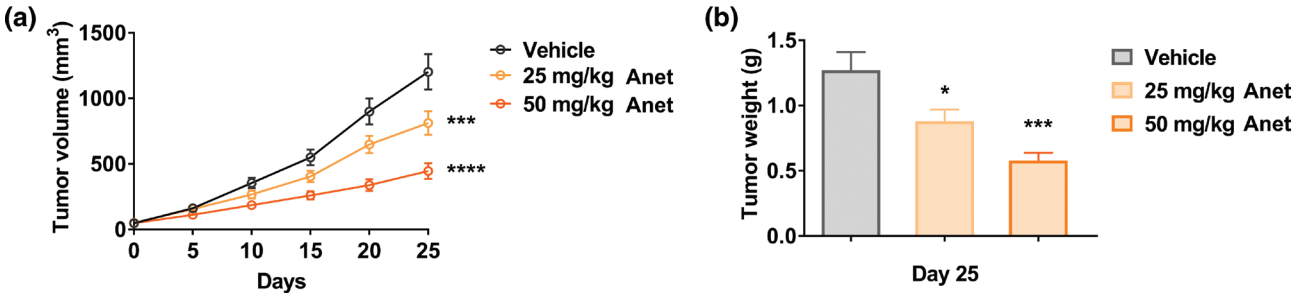

Fig. 5. Anethole inhibited the progression of A549 tumor *in vivo*. A549 tumor-bearing mice were treated by vehicle, 25, or 50 mg/kg anethole. The indexes of tumor volume (a) and weight at the end point (b) were measured. $n = 7$ for each group. Error bar represents SEM. $^{*}P < 0.05$, $^{***}P < 0.001$, and $^{****}P < 0.0001$.

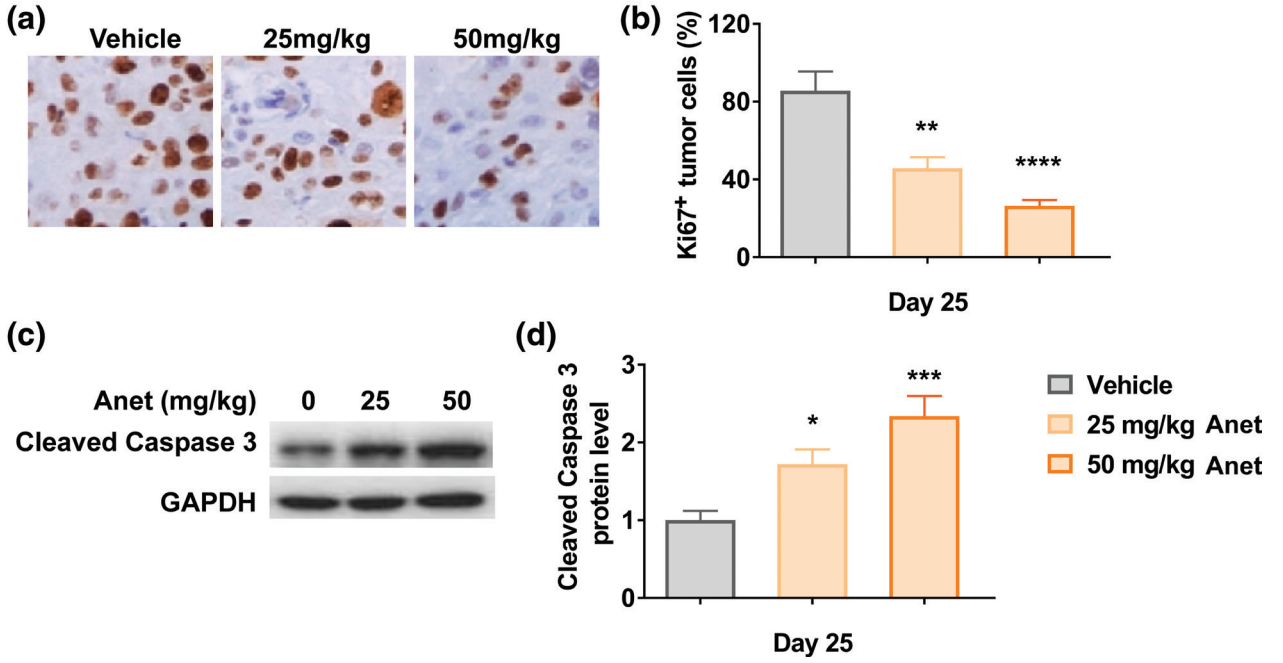

Fig. 6. Anethole inhibited the proliferation and promoted the apoptosis of A549 tumor *in vivo*. A549 tumor-bearing mice were treated by vehicle, 25, or 50 mg/kg anethole. The tumors were harvested at day 25 to analyze the expression levels of Ki67 (a and b) by IHC and cleaved Caspase 3 (c and d) by Western blot. $n = 7$ for each group. Error bar represents SEM. $^{*}P < 0.05$, $^{***}P < 0.01$, $^{***}P < 0.001$, and $^{****}P < 0.0001$.

Anethole inhibited the proliferation and promoted the apoptosis

Furthermore, we determined the proliferation and apoptosis of xenografted tumor cells, via determining the level of Ki67, a marker for cell proliferation, as well as cleaved Caspase 3, a apoptosis-related protein. Data implied that the percentage of Ki67 positive tumor cells was significantly lower (Fig. 6a, b), and the protein level of cleaved caspase 3 was obviously higher (Fig. 6c, d) in Aent-treated group than control group. In brief, anethole markedly inhibited the proliferation and enhanced the apoptosis of A549 tumor in vivo.

Discussion

Nowadays, lung cancer remains to be the most deadly cancer worldwide, and it is urgent to develop more powerful therapeutic options, especially chemotherapies, to enhance patients' 5-year survival rate (14, 15). Anethole is a natural ingredient existing in multiple spices, and studies prove that it has powerful antitumor function in breast cancer, prostate cancer, and other chronic diseases (10, 11, 13). In the present study, we found that anethole suppressed proliferation of lung cancer cells cultured *in vitro*. Anethole also promoted apoptosis of lung cancer cells via enhancing the expression of proapoptotic proteins as well as reducing

the expression of antiapoptotic proteins *in vitro*. Furthermore, we demonstrated that AKT and STAT3 signaling might be involved in the molecular mechanism underlying the antitumor effects of anethole on lung cancer cells *in vitro*. The inhibitory effects of anethole on lung cancer cells were further validated *in vivo*, and the results of which were consistent with those obtained *in vitro*. These findings were similar with previous studies. Elkady reported that anethole inhibited the proliferation of prostate cancer cell line via the induction of G2/M phase arrest, apoptosis, and the suppression of NF-κB nuclear localization (11). Another study indicated the similar inhibitory effects on human breast cancer cells manifested by suppressed cell survival, which increased apoptosis in an estrogen receptor independent manner (10).

PI3K/Akt signaling pathway plays important roles in cellular events, including cell proliferation, growth, and migration (16). This pathway has been demonstrated to be upregulated and lead to increased cell proliferation and survival in many malignant tumors, for example, melanoma, gastric cancer, myeloma, and lung cancer (17–21). PI3K/Akt upregulation has been recorded to contribute to radiotherapy resistance of NSCLC, and specific pathway inhibitors function substantially sensitizes cancer cells to radiotherapy (16).

Another signaling pathway involved in the tumorigenesis is STAT3, which is essential to many cellular functions, such as proliferation, angiogenesis, invasion, and metastasis (22, 23). Abnormal activation of STAT3 has been referred to in malignant tumors involving brain, kidney, prostate, and lung (24–26). Song et al. indicated that NSD2-mediated STAT3 methylation-activated STAT3 pathway eventually promoted tumor angiogenesis (27). Activated STAT3 also correlates with drug resistance in lung cancer cells. Previous studies illustrated JAK/STAT3 signaling is significantly increased in cisplatin-resistant lung cancer cells, and the inhibition of Ataxia Telangiectasia Mutated targeting JAK/STAT3 signaling could retard the metastatic behavior of cancer cells (28). STAT3 pathway has been highlighted as a therapeutic target with promising potential for cancers, including lung cancer (26). In brief, PI3K/Akt and STAT3 are promising targets for lung cancer therapy. To be consistent with the previous studies regarding PI3K/Akt and STAT3 pathways, we also found the decreased expression of related effectors is positively correlated with reduced cell proliferation of lung cancer cells.

Anethole has been stated to inhibit cancer malignancy via the suppression of the chemokine CXCR4 powerfully without cytotoxicity in prostate cancer cells in vitro (29). The downregulation of Akt is involved in the antimetastatic process of anethole to prostate cancer cells (30). Choo et al. mentioned the antimetastatic activity of anethole on human fibrosarcoma tumor cells via the inhibition of AKT/mitogen-activated protein kinase/NF-κB signaling (13). Our study demonstrates that anethole possesses inhibitory effect on lung cancer cells using in vitro and in vivo experiments and indicates its negative modulation of PI3K/Akt and STAT3 signaling pathways.

Several limitations should be noted in the present study. We did not explore thoroughly the effects of anethole on metastatic and invasive capacities, which are also critic characteristics of advanced NSCLC. The concrete molecular mechanisms were not further validated. Loss-function and gain-function assays should be designed and performed in the future study. Besides, the safety and cytotoxicity would also be investigated in our future work.

Conclusions

Taken together, our study implied that anethole exerts antitumor potentialities on lung cancer cells via retarding proliferation and promoting apoptosis possibly through AKT and STAT3 signaling in vivo and in vitro. We confidently believe that anethole is a promising chemotherapeutic drug to lung cancer in future.

Acknowledgment

None.

Conflict of interest and funding

The authors have no conflict of interest to declare. This work was supported by Medical Research Funding in Haryana (cj.v523).

References

1. Sharma P, Mehta M, Dhanjal DS, Kaur S, Gupta G, Singh H, et al. Emerging trends in the novel drug delivery approaches for the treatment of lung cancer. Chem Biol Interact. 2019; 309: 108720. doi: 10.1016/j.cbi.2019.06.033
2. Siegel RL, Miller KD, Jemal A. Cancer statistics, 2020. CA Cancer J Clin. 2020; 70(1): 7–30. doi: 10.3322/caac.21590
3. Malyla V, Paudel KR, Shukla SD, Donovan C, Wadhwa R, Pickles S, et al. Recent advances in experimental animal models of lung cancer. Future Med Chem. 2020; 12(7): 567–70. doi: 10.4155/fmc-2019-0338
4. Rolfo C, Giovannetti E, Hong DS, Bivona T, Raez LE, Bronte G, et al. Novel therapeutic strategies for patients with NSCLC that do not respond to treatment with EGFR inhibitors. Cancer Treat Rev. 2014; 40(8): 990–1004. doi: 10.1016/j.ctrv.2014.05.009
5. Klastersky J, Awada A. Milestones in the use of chemotherapy for the management of non-small cell lung cancer (NSCLC). Crit Rev Oncol Hematol. 2012; 81(1): 49–57. doi: 10.1016/j.critrevonc.2011.02.002
6. Islam KM, Anggondowati T, Deviany PE, Ryan JE, Fetrick A, Bagenda D, et al. Patient preferences of chemotherapy treatment options and tolerance of chemotherapy side effects in advanced stage lung cancer. BMC Cancer. 2019; 19(1): 835. doi: 10.1186/s12885-019-6054-x
7. Peng Z, Wu WW, Yi P. The efficacy of ginsenoside Rg3 combined with first-line chemotherapy in the treatment of advanced non-small cell lung cancer in China: a systematic review and

meta-analysis of randomized clinical trials. Front Pharmacol. 2020; 11: 630825. doi: 10.3389/fphar.2020.630825
8. von Plessen C. Improving chemotherapy for patients with advanced non-small cell lung cancer. Clin Respir J. 2011; 5(1): 60–1. doi: 10.1111/j.1752-699X.2010.00199.x
9. Aprotosoaie AC, Costache, II, Miron A. Anethole and its role in chronic diseases. Adv Exp Med Biol. 2016; 929: 247–67. doi: 10.1007/978-3-319-41342-6_11
10. Chen CH, deGraffenried LA. Anethole suppressed cell survival and induced apoptosis in human breast cancer cells independent of estrogen receptor status. Phytomedicine. 2012; 19(8–9): 763–7. doi: 10.1016/j.phymed.2012.02.017
11. Elkady AI. Anethole inhibits the proliferation of human prostate cancer cells via induction of cell cycle arrest and apoptosis. Anticancer Agents Med Chem. 2018; 18(2): 216–36. doi: 10.2174/1871520617666170725165717
12. Chainy GB, Manna SK, Chaturvedi MM, Aggarwal BB. Anethole blocks both early and late cellular responses transduced by tumor necrosis factor: effect on NF-kappaB, AP-1, JNK, MAPKK and apoptosis. Oncogene. 2000; 19(25): 2943–50. doi: 10.1038/sj.onc.1203614
13. Choo EJ, Rhee YH, Jeong SJ, Lee HJ, Kim HS, Ko HS, et al. Anethole exerts antimetatstaic activity via inhibition of matrix metalloproteinase 2/9 and AKT/mitogen-activated kinase/nuclear factor kappa B signaling pathways. Biol Pharm Bull. 2011; 34(1): 41–6. doi: 10.1248/bpb.34.41
14. Nasim F, Sabath BF, Eapen GA. Lung cancer. Med Clin North Am. 2019; 103(3): 463–73. doi: 10.1016/j.mcna.2018.12.006
15. Herbst RS, Morgensztern D, Boshoff C. The biology and management of non-small cell lung cancer. Nature. 2018; 553(7689): 446–54. doi: 10.1038/nature25183
16. Wanigasooriya K, Tyler R, Barros-Silva JD, Sinha Y, Ismail T, Beggs AD. Radiosensitising cancer using phosphatidylinositol-3-kinase (PI3K), protein kinase B (AKT) or mammalian target of rapamycin (mTOR) inhibitors. Cancers (Basel). 2020; 12(5): 1278. doi: 10.3390/cancers12051278
17. Lee YJ, Kim WI, Park TH, Bae JH, Nam HS, Cho SW, et al. Upregulation of DJ-1 expression in melanoma regulates PTEN/AKT pathway for cell survival and migration. Arch Dermatol Res. 2021; 313(7): 583–591. doi: 10.1007/s00403-020-02139-1
18. Xiao S, Li S, Yuan Z, Zhou L. Pyrroline-5-carboxylate reductase 1 (PYCR1) upregulation contributes to gastric cancer progression and indicates poor survival outcome. Ann Transl Med. 2020; 8(15): 937. doi: 10.21037/atm-19-4402
19. John L, Krauth MT, Podar K, Raab MS. Pathway-directed therapy in multiple myeloma. Cancers (Basel). 2021; 13(7): 1668. doi: 10.3390/cancers13071668
20. Yu H, Tian L, Yang L, Liu S, Wang S, Gong J. Knockdown of SNORA47 inhibits the tumorigenesis of NSCLC via mediation of PI3K/Akt signaling pathway. Front Oncol. 2021; 11: 620213. doi: 10.3389/fonc.2021.620213
21. Song M, Bode AM, Dong Z, Lee MH. AKT as a Therapeutic target for cancer. Cancer Res. 2019; 79(6): 1019–31. doi: 10.1158/0008-5472.CAN-18-2738
22. Darnell JE, Jr. The JAK-STAT pathway: summary of initial studies and recent advances. Recent Prog Horm Res. 1996; 51: 391–403; discussion 4.
23. Gao P, Niu N, Wei T, Tozawa H, Chen X, Zhang C, et al. The roles of signal transducer and activator of transcription factor 3 in tumor angiogenesis. Oncotarget. 2017; 8(40): 69139–61. doi: 10.18632/oncotarget.19932
24. Schaefer LK, Ren Z, Fuller GN, Schaefer TS. Constitutive activation of Stat3alpha in brain tumors: localization to tumor endothelial cells and activation by the endothelial tyrosine kinase receptor (VEGFR-2). Oncogene. 2002; 21(13): 2058–65. doi: 10.1038/sj.onc.1205263
25. Li S, Priceman SJ, Xin H, Zhang W, Deng J, Liu Y, et al. Icaritin inhibits JAK/STAT3 signaling and growth of renal cell carcinoma. PLoS One. 2013; 8(12): e81657. doi: 10.1371/journal.pone.0081657
26. Lee H, Jeong AJ, Ye SK. Highlighted STAT3 as a potential drug target for cancer therapy. BMB Rep. 2019; 52(7): 415–23. doi: 10.5483/BMBRep.2019.52.7.152
27. Song D, Lan J, Chen Y, Liu A, Wu Q, Zhao C, et al. NSD2 promotes tumor angiogenesis through methylating and activating STAT3 protein. Oncogene. 2021; 40(16): 2952–67. doi: 10.1038/s41388-021-01747-z
28. Shen M, Xu Z, Xu W, Jiang K, Zhang F, Ding Q, et al. Inhibition of ATM reverses EMT and decreases metastatic potential of cisplatin-resistant lung cancer cells through JAK/STAT3/PD-L1 pathway. J Exp Clin Cancer Res. 2019; 38(1): 149. doi: 10.1186/s13046-019-1161-8
29. Rhee YH, Chung PS, Kim SH, Ahn JC. CXCR4 and PTEN are involved in the anti-metastatic regulation of anethole in DU145 prostate cancer cells. Biochem Biophys Res Commun. 2014; 447(4): 557–62. doi: 10.1016/j.bbrc.2014.01.121
30. Ha B, Ko H, Kim B, Sohn EJ, Jung JH, Kim JS, et al. Regulation of crosstalk between epithelial to mesenchymal transition molecules and MMP-9 mediates the antimetastatic activity of anethole in DU145 prostate cancer cells. J Nat Prod. 2014; 77(1): 63–9. doi: 10.1021/np4006376

***Maddula Venkateswarulu**
MM Education Complex
Mullana, Haryana 133207
India
Email: maddula103@outlook.com